

# Bistetracene: An Air-Stable, High-Mobility Organic Semiconductor with Extended Conjugation

Lei Zhang,<sup>†</sup> Alexandr Fonari,<sup>‡</sup> Yao Liu,<sup>†</sup> Andra-Lisa M. Hoyt,<sup>†</sup> Hyunbok Lee,<sup>†</sup> Devin Granger,<sup>§</sup> Sean Parkin,<sup>§</sup> Thomas P. Russell,<sup>†</sup> John E. Anthony,<sup>§</sup> Jean-Luc Brédas,<sup>‡</sup> Veaceslav Coropceanu,<sup>‡</sup> and Alejandro L. Briseno<sup>\*,†</sup>

<sup>†</sup>Department of Polymer Science & Engineering, Conte Polymer Research Center, University of Massachusetts, Amherst, Massachusetts 01003, United States

<sup>‡</sup>School of Chemistry & Biochemistry and Center for Organic Photonics and Electronics, Georgia Institute of Technology, Atlanta, Georgia 30332-0400, United States

<sup>§</sup>Department of Chemistry, University of Kentucky, Lexington, Kentucky 40506, United States

## Supporting Information

**ABSTRACT:** We report the synthesis and characterization of “bistetracene”, an unconventional, linearly extended conjugated core with eight fused rings. The annellation mode of the system allows for increased stability of the conjugated system relative to linear analogues due to the increased number of Clar aromatic sextets. By attaching the appropriate solubilizing substituents, efficient molecular packing with large transfer integrals can be obtained. The electronic structure calculations suggest these large polycyclic aromatic hydrocarbons (PAHs) exhibit excellent intrinsic charge transport properties. Charge carrier mobilities as large as  $6.1 \text{ cm}^2 \text{ V}^{-1} \text{ s}^{-1}$  and current on/off ratios of  $10^7$  were determined experimentally for one of our compounds. Our study provides valuable insight into the design of unconventional semiconductor compounds based on higher PAHs for use in high-performance devices.

Polyacenes with linearly annellated benzene units have received much attention in both experimental and theoretical studies because of their unique electronic structures.<sup>1</sup> In particular, they have been closely examined as semiconductor materials in organic field-effect transistors (OFETs) due to their relatively high charge-carrier mobility.<sup>1b,c</sup> Since increased conjugation length could be beneficial for electronic coupling and reducing reorganization energies in the solid state, chemists have been pursuing acenes larger than pentacene, one of the most popular and well-studied materials for organic devices.<sup>2</sup> However, it is becoming clear that the higher acenes and periacenes suffer from reduced stability, due to the zigzag peripheries, leading to low resonance stabilization, small band gaps, and high reactivity.<sup>3</sup> Although significant progress has been made in the development of higher acenes, only a handful have been successfully synthesized and characterized due to the multiple synthetic steps, poor solubility, and extreme instability (sensitivity to light, oxygen, and polymerization).<sup>4</sup> One avenue to increase solubility and kinetically enhance stability has been the addition of protecting substituents, such as phenyl, arylthio, or silylethylene, at peri-positions on the periphery of the

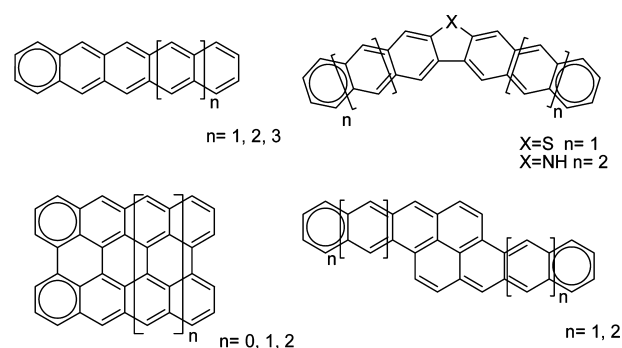


**Figure 1.** Chemical structures of representative higher polyacenes with different modes of annellation and Clar sextets.

conjugated acene frameworks, although many of the bulkier substituents disrupt the  $\pi$ -stacking motif, inhibiting charge transport.<sup>5</sup> Hence, there are opportunities for exploration in the design and characterization of unconventional polycyclic aromatic frameworks and their use in device applications.<sup>6</sup>

In general, the properties and stability of large polycyclic aromatic hydrocarbons (PAHs) strongly depend on the mode of ring annellation and the topology of their  $\pi$ -electron systems, which are usually associated with the resonance stabilization energy in large PAHs.<sup>7</sup> For example, the stability of polyacenes can be improved by changing the linearity of a condensed array to an angular analogue, such as V-shape and triangular geometries (Figure 1).<sup>8</sup> The simple interpretation of the stability of these compounds can be obtained in the framework of the aromatic Clar sextet model, which states that a molecule with more benzenoid sextets increases the overall aromatic stabilization energy.<sup>1d</sup> These compounds have at least two sextets, rendering them more stable than linear analogues with only one sextet.<sup>1d</sup> Recently, Wudl succeeded at preparing stable angular dinaphthocarbazoles with seven fused rings for solution-processed OFETs with mobilities up to  $0.055 \text{ cm}^2 \text{ V}^{-1} \text{ s}^{-1}$ .<sup>8a</sup> In a separate study, Okamoto reported a V-shaped semiconductor with mobility as large as  $9.5 \text{ cm}^2 \text{ V}^{-1} \text{ s}^{-1}$ .<sup>8c</sup> We recently reported a series of soluble

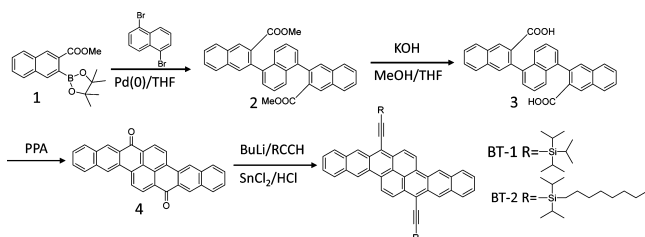
Received: April 11, 2014

Published: May 6, 2014

two-dimensional (2-D) small graphene-like fragments that possess relatively large band gaps due to an increase in the number of Clar sextets.<sup>9</sup> Furthermore, the molecular packing and electronic structure of these compounds were greatly affected by the aspect ratio between length and width of the aromatic cores.<sup>9a</sup> These interesting results, together with the application in organic devices, prompted us to investigate even larger conjugated PAH analogues. Here, we report the synthesis of solution-processable, air-stable organic semiconductors with extended conjugation, namely, “bistetracenes”, and discuss their electronic/molecular structures, crystal packing, and performance in OFETs.

Scheme 1 shows the synthesis of soluble bistetracene. Diketone **4** is the key intermediate compound for soluble

### Scheme 1. Synthesis of Soluble Bistetracene



bistetracene, which was synthesized by Clar in 1949.<sup>10</sup> In this Communication, we develop a modified procedure to synthesize bistetracene quinone with high overall yield. Suzuki coupling between the boronic ester **1** and 1,5-dibromonaphthalene produced **2**, which was subsequently hydrolyzed to dicarboxylic acid **3** in high yield. The desired diketone **4** was then obtained from **3** under polyphosphoric acid (PPA). Lithiation of alkyl-substituted silylacetylene in THF with BuLi to form its anion and subsequent treatment with diketone **4** gave the relative alcohol derivatives, followed by reductive aromatization with SnCl<sub>2</sub>, affording the desired products. In our study, **BT-1** with triisopropylsilyl acetylene (TIPS) substituent and **BT-2** with *N*-octyldiisopropylsilyl acetylene (NODIPSA) substituent are synthesized. These compounds are purified via silica gel column chromatography and recrystallization from hexane.

The UV/vis absorption spectra of the compounds were measured in chloroform solution (see Figure 2 for **BT-2**). At

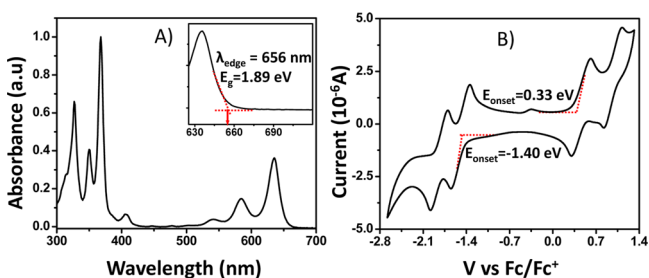


**Figure 2.** (A) UV/vis absorption spectra of **BT-2** in chloroform solution. (B) CV of **BT-2** in chlorobenzene with TBAPF<sub>6</sub> as supporting electrolyte.

short wavelengths (up to 550 nm), the compounds show well-defined peaks with intense absorption. The vibronic peaks with weak absorption in the range of 550–635 nm are characteristic of the acene family.<sup>11</sup> The lowest optical band peaks at ~635 nm (1.95 eV). Time-dependent density functional theory (TD-DFT) calculations for **BT-1** were performed with the long-range

corrected  $\omega$ B97 functional using the 6-31G\*\* basis set. The range-separation parameter  $\omega$  was optimized following the ionization potential (IP) tuning procedure.<sup>12</sup> These TD-DFT calculations yield a value of 1.87 eV for the first optical band, corresponding essentially to a HOMO-to-LUMO excitation (see SI for details).

Cyclic voltammetry (CV) studies were performed in chlorobenzene with 0.1 M TBAPF<sub>6</sub> as the supporting electrolyte at a scan rate of 100 mV/s, and onset oxidation potentials were determined relative to Fc/Fc<sup>+</sup> (4.8 eV). The CVs of **BT-1** and **BT-2** exhibit two well-defined, reversible oxidation and reduction waves. The first half-wave reduction–oxidation potentials are –0.76, 1.08 V for **BT-1** and –0.77, 1.09 V for **BT-2**. According to their onset potentials, the IPs and electron affinities (EAs) were estimated at 5.11 and 3.40 eV for **BT-1** and 5.13 and 3.40 eV for **BT-2**, comparable to those of TIPS-pentacene.<sup>13</sup> The optical gap extracted from the onset of the optical spectra is 1.89 eV. DFT calculations also confirm that, as expected, the energies of the frontier orbitals in both systems are nearly identical (see SI). The IPs measured by ultraviolet photoelectron spectroscopy (UPS) (see SI) of **BT-1** and **BT-2** were 5.02 and 4.88 eV, respectively. A small deviation of IPs between **BT-1** and **BT-2** (0.14 eV) might be attributed to their different packing motifs in thin films. We also monitored UV/vis absorption over time for **BT-1** in chloroform and found that it has a half-life time of 4 days (see SI), making it ~200 times more stable than pentacene.<sup>14</sup> These data thus point out that these compounds are very stable.

The crystal structures of **BT-1** and **BT-2** were determined by single-crystal X-ray diffraction (Figure 3). Both **BT-1** and **BT-2**

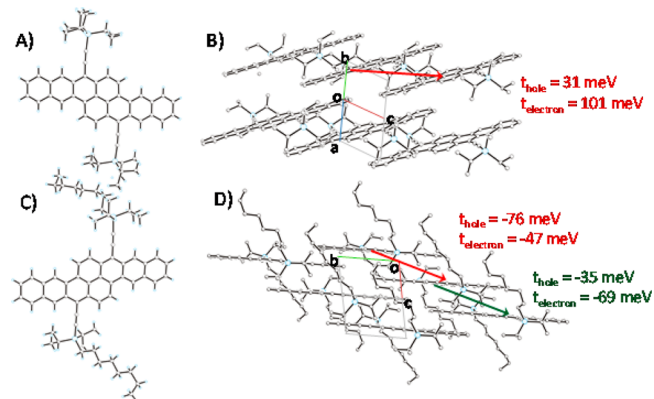


**Figure 3.** Crystal structure and molecular packing of (A,B) **BT-1** (slipped 1-D) and (C,D) **BT-2** (interacting 2-D) with indication of the largest calculated electronic couplings.

crystals are triclinic, space group  $P\bar{1}$ . Although both structures have two molecules per unit cell, they differ in that the asymmetric unit of **BT-1** has two half-molecules (sitting on inversion centers), whereas **BT-2** has a single whole molecule per asymmetric unit. As shown in Figure 3, **BT-1** exhibits a slipped one-dimensional (1-D)  $\pi$ -stacking motif, similar to that observed for some soluble pentacene derivatives.<sup>15</sup> The interplanar distance in **BT-1** is ~3.37 Å, while the center-to-center distance between two adjacent molecules is ~8.98 Å. The peripheral C-atoms in the 1-D stacks of **BT-1** are separated by at least 3.8 Å from adjacent stacks, larger than the van der Waals radii for adjacent C-atoms, leading to poor electronic coupling between two adjacent stacks. By changing the substituent to the larger alkyl groups, the  $\pi$ -stacking motif in **BT-2** changed to an

interacting 2-D packing arrangement with close intrastack contacts of 3.35 Å. A few atoms within the stacks of BT-2 are separated by as little as 3.6 Å, allowing non-negligible electronic coupling between adjacent stacks. Due to the presence of two translationally inequivalent molecules (i.e., molecules related by different inversion centers), the stacks in BT-2 are characterized by two alternating intermolecular center-to-center distances of 8.59 and 8.01 Å between adjacent molecules. The introduction of long alkyl groups tends to reduce the distance between the different stacks. This is consistent with the stronger intermolecular van der Waals interactions among the longer alkyl groups (“zipper effect”), which result in tighter packing in the solid state.<sup>16</sup> The other important observation is the slight twisting of the acene core of BT-2 (torsion angle 4.8°), which likely arises to alleviate strain in crystal packing due to the bulky substituents.

Bottom contact field-effect transistors were fabricated, using as substrate octadecyl trichlorosilane (ODTS)-treated Si/SiO<sub>2</sub>. The source and drain electrodes were prepared by gold evaporation, with channel length and width of 50 μm. The OFET devices were measured under ambient conditions using a standard probe station. Transfer and output characteristics are shown in Figure 4A,B. The average performance of BT-1 devices was 0.28 cm<sup>2</sup> V<sup>-1</sup> s<sup>-1</sup>, with threshold voltage  $V_{th} = -5$  V and current on/off ratio of  $\sim 10^5$ . Among the results, the best mobility was 0.4 cm<sup>2</sup> V<sup>-1</sup> s<sup>-1</sup>, with  $V_{th} = 6$  V and current on/off ratio of  $10^5$ . However, for BT-2, the average mobility is  $\sim 3.90$  cm<sup>2</sup> V<sup>-1</sup> s<sup>-1</sup>, with  $V_{th} = -5$  V and current on/off ratio of  $\sim 10^6$  over 10 individual devices. The best mobility is measured to be 6.1 cm<sup>2</sup> V<sup>-1</sup> s<sup>-1</sup>. Thus, BT-2 exhibits excellent device performance, higher than that of materials with the similar 2-D packing motifs.<sup>1b,c</sup> We note that, due to contact effects, the linear regime mobilities were slightly lower than the saturated mobilities (SI).

To test the device stability, we prepared single-crystal transistors based on BT-2 and stored them in laboratory

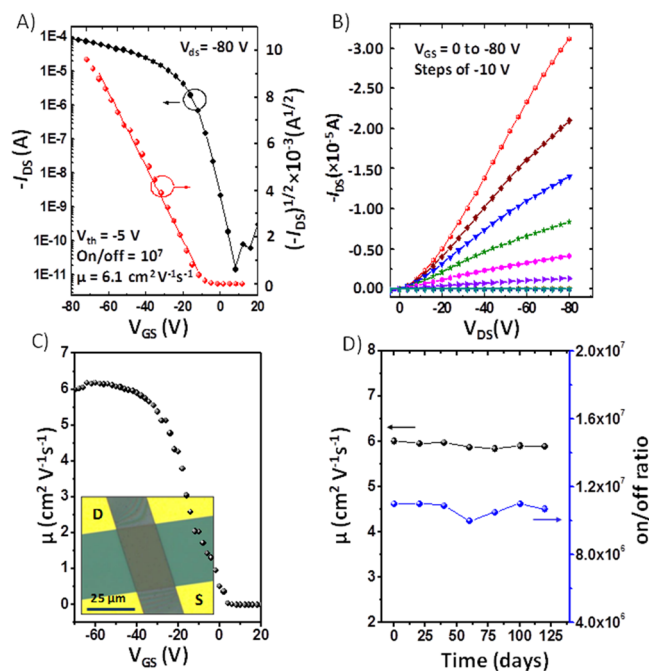


**Figure 4.** Single-crystal transistor characteristics of BT-2. (A) Transfer characteristics in the saturated region. (B) Output characteristics at different gate voltages. (C) Plot showing dependence of mobility on gate voltage. (D) Device stability test over several months.

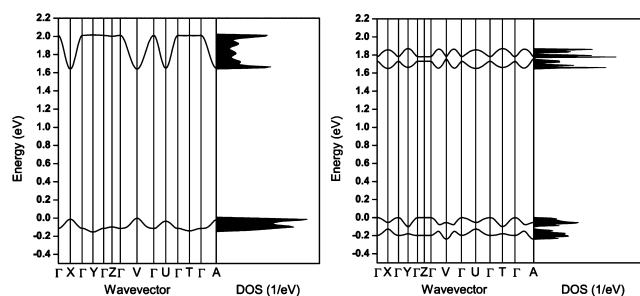


**Figure 5.** Band structure for the relaxed geometry of BT-1 (left) and BT-2 (right). The points of high symmetry in the first Brillouin zone are  $\Gamma = (0,0,0)$ ,  $X = (0.5,0,0)$ ,  $Y = (0,0.5,0)$ ,  $Z = (0,0,0.5)$ ,  $V = (0.5,0.5,0)$ ,  $U = (0.5,0,0.5)$ ,  $T = (0,0.5,0.5)$ , and  $A = (0.5,0.5,0.5)$ , all in crystallographic coordinates. The zero of energy corresponds to the top of the valence band.

drawers. The devices were periodically tested under ambient conditions for more than 4 months. During this period, only small fluctuations in the mobilities and current on/off ratios were measured.

To understand the intrinsic charge transport properties of BT-1 and BT-2, we investigated their electronic band structures via DFT at the B3LYP/6-21G level of theory (Figure 5). In the case of BT-1, the valence and conduction bandwidths are 0.17 and 0.4 eV, respectively. The corresponding transfer integrals for holes and electrons are estimated as 31 and 101 meV (Figure 3B); in the framework of a 1-D tight-binding model, such transfer integrals would result in valence and conduction bandwidths of 0.12 and 0.4 eV, respectively, in good agreement with those from the periodic boundary conditions calculations. As a consequence of relatively large transfer integrals, the effective masses along the stacking direction are small,  $1.07m_0$  ( $m_0$  is the electron mass in vacuum) for holes and  $0.53m_0$  for electrons (Table S1). For the sake of comparison, we note that the effective masses for holes and electrons in pentacene are  $1.60m_0$  and  $1.45m_0$ , respectively.<sup>17</sup> Interstack electronic couplings were found to be small, i.e., 3 and 1 meV for holes and electrons, respectively.

In BT-2, the valence and conduction bands consist of two subbands arising from the interaction of the HOMO and LUMO levels, respectively, of the two translationally inequivalent molecules present in the unit cell. The overall valence and conduction bandwidths are estimated to be 0.22 and 0.20 eV. As a result of two alternating intermolecular distances, the electronic coupling along the stacks is characterized by two transfer integrals,  $t_1$  and  $t_2$  ( $-35$  and  $-76$  meV for holes, and  $-69$  and  $-47$  meV for electrons). The band structure calculations yield  $1.05m_0$  and  $0.97m_0$ , respectively, for hole and electron effective masses along stacking directions. A tight-binding model (but with two sites per unit cell) can be employed to rationalize the band structure for this system as well.<sup>18</sup> According to this model, the bandwidths in BT-2 are given by  $2(|t_1| + |t_2|)$ . The tight-binding estimates of 0.22 and 0.23 eV for the widths of the valence and conduction bands compare well with the above values derived from band-structure calculations. According to the same tight-binding model, the effective masses for charge carriers can be estimated as  $m_{eff} = \hbar^2/2t_{eff}d_{av}^2$ , where  $t_{eff} = 2|t_1t_2|/(|t_1| + |t_2|)$  and  $d_{av}$  is the average intermolecular distance along the stack.<sup>18a</sup> The model yields nearly equal values for the effective transfer integrals for holes and electrons (48 vs 55 meV), explaining why both types of carriers in BT-2 possess comparable effective masses. We note that the tight-binding calculations predict for the effective mass of holes in BT-2 a value that is

~30% smaller than in the case of BT-1, in contrast with the band-structure calculations showing that the effective masses for holes in both crystals are almost equal. Unlike BT-1, non-negligible electronic couplings were found between stacks in BT-2, 14 and 4 meV for holes and electrons, respectively. Despite a very large difference in the interstack electronic couplings, the hole effective masses along the interstack direction in both crystals are similar (see SI). This result can be explained by the fact that the effective mass (see above) also depends on the hopping distance; the interstack distance in BT-1 is larger than in BT-2. We note, however, that the electronic interaction between stacks, except for holes in BT-2, is expected to be easily diminished by already moderate defects that is always present in actual crystals. Overall, the electronic-structure calculations suggest that BT-1 and BT-2 should exhibit excellent intrinsic charge transport properties for both holes and electrons along the stacking directions. Moderate transport properties are also expected for holes along the interstack direction in BT-2.

In summary, we have described a straightforward synthesis of soluble bistetracene derivatives that show attractive properties, such as solution processability, air stability, low-energy band gaps, and high carrier mobilities. The OFET measurements and electronic-structure calculations demonstrate that these acenes also exhibit excellent intrinsic charge transport properties. Our study indicates that this annellation mode with an additional Clar sextet significantly increases the stability of this class of extended conjugated semiconductors and opens new opportunities to explore these materials in mainstream applications such as bulk heterojunction solar cells and large-area, roll-to-roll solution-processable transistors. Further studies on the comprehensive synthesis and structure–property relationships of even larger conjugated cores are now in progress.

## ■ ASSOCIATED CONTENT

### 📄 Supporting Information

Experimental details, synthesis, characterization, device fabrication, theoretical studies, and crystal data. This material is available free of charge via the Internet at <http://pubs.acs.org>.

## ■ AUTHOR INFORMATION

### Corresponding Author

[abriseno@mail.pse.umass.edu](mailto:abriseno@mail.pse.umass.edu)

### Notes

The authors declare no competing financial interest.

## ■ ACKNOWLEDGMENTS

Collaboration between the UMass (L.Z., H.L., A.L.B.) and Georgia Tech (A.F., V.C., J.-L.B.) groups is supported by the Office of Naval Research awards N000141110636 and N000141110211. Y.L. and T.P.R. acknowledge support by the Department of Energy supported Energy Frontier Research Center at the University of Massachusetts (DOE DE-SC0001087). D.G. and J.E.A. acknowledge support from the Office of Naval Research award N000141110329. S.P. acknowledges the NSF MRI program (CHE-0319176). We acknowledge Y. Zhang for fabricating OFET device structures for this work.

## ■ REFERENCES

(1) (a) Bendikov, M.; Wudl, F.; Perepichka, D. F. *Chem. Rev.* **2004**, *104*, 4891. (b) Anthony, J. E. *Angew. Chem., Int. Ed.* **2008**, *47*, 452. (c) Anthony, J. E. *Chem. Rev.* **2006**, *106*, 5028. (d) Clar, E. *Polycyclic Hydrocarbons*; Academic Press: New York, 1964; Vol. 1.

- (2) (a) Zade, S.; Bendikov, M. *Angew. Chem., Int. Ed.* **2010**, *49*, 4012. (b) Winkler, M.; Houk, K. N. *J. Am. Chem. Soc.* **2007**, *129*, 1805.
- (3) (a) Sun, Z.; Ye, Q.; Chi, C.; Wu, J. *Chem. Soc. Rev.* **2012**, *41*, 7857. (b) Jiang, D. F.; Dai, S. *Chem. Phys. Lett.* **2008**, *466*, 72.
- (4) (a) Mondal, R.; Tönshoff, C.; Khon, D.; Neckers, D. C.; Bettinger, H. F. *J. Am. Chem. Soc.* **2009**, *131*, 14281. (b) Ehrlich, S.; Bettinger, H. F.; Grimme, S. *Angew. Chem., Int. Ed.* **2013**, *52*, 10892. (c) Tönshoff, C.; Bettinger, H. F. *Angew. Chem., Int. Ed.* **2010**, *49*, 4125. (d) Watanabe, M.; Chen, K.; Chang, Y. J.; Chow, T. J. *Acc. Chem. Res.* **2013**, *46*, 1606. (e) Zade, S. S.; Zamoshchik, N.; Reddy, A. R.; Fridman-Marueli, G.; Sheberla, D.; Bendikov, M. *J. Am. Chem. Soc.* **2011**, *133*, 10803.
- (5) (a) Payne, M. M.; Parkin, S. R.; Anthony, J. E. *J. Am. Chem. Soc.* **2005**, *127*, 8028. (b) Chun, D.; Cheng, Y.; Wudl, F. *Angew. Chem., Int. Ed.* **2008**, *47*, 8380. (c) Kaur, I.; Stein, N. N.; Kopreski, R. P.; Miller, G. P. *J. Am. Chem. Soc.* **2009**, *131*, 3424. (d) Purushothaman, B.; Bruzek, M.; Parkin, S. R.; Miller, A.; Anthony, J. E. *Angew. Chem., Int. Ed.* **2011**, *50*, 7013. (e) Xiao, J. C.; Duong, H. M.; Liu, Y.; Shi, W. X.; Li, G.; Li, S. Z.; Liu, X. W.; Ma, J.; Wudl, F.; Zhang, Q. C. *Angew. Chem., Int. Ed.* **2012**, *51*, 6094.
- (6) (a) Watanabe, M.; Chang, Y. J.; Liu, S. W.; Chao, T. H.; Goto, K.; Islam, M. M.; Yuan, C. H.; Tao, U. T.; Shinmyozu, T.; Chow, T. J. *Nat. Chem.* **2012**, *4*, 574. (b) Purushothaman, B.; Parkin, S.; Kendrick, M. J.; David, D.; Ward, J. W.; Yu, L.; Stingelin, N.; Jurchescu, O. D.; Ostroverkhova, O.; Anthony, J. E. *Chem. Commun.* **2012**, *48*, 8261. (c) Winzenberg, K. N.; Kempainen, P.; Fanchini, G.; Bown, M.; Collis, G. E.; Forsyth, C. M.; Hegedus, K.; Birendra Singh, T.; Watkins, S. E. *Chem. Mater.* **2009**, *21*, 5701. (d) Yamashita, M.; Kuzuhara, D.; Aratani, N.; Yamada, H. *Chem.—Eur. J.* **2014**, DOI: 10.1002/chem.201304997.
- (7) (a) Gutzler, R.; Perepichka, D. F. *J. Am. Chem. Soc.* **2013**, *135*, 16585. (b) Kastler, M.; Schmidt, J.; Pisula, W.; Sebastiani, D.; Müllen, K. *J. Am. Chem. Soc.* **2006**, *128*, 9526. (c) Wu, J.; Pisula, W.; Müllen, K. *Chem. Rev.* **2007**, *107*, 718. (d) Debije, M. G.; Piris, J.; de Haas, M. P.; Warman, J. M.; Tomović, Z.; Simpson, C. D.; Watson, M. D.; Müllen, K. *J. Am. Chem. Soc.* **2004**, *126*, 4641.
- (8) (a) Pho, T. V.; Yuen, J. D.; Kurzman, J. A.; Smith, B. G.; Miao, M. S.; Walker, W. T.; Seshadri, R.; Wudl, F. *J. Am. Chem. Soc.* **2012**, *134*, 18185. (b) Alonso, J. M.; Diaz-Álvarez, A. D.; Criado, A.; Pérez, D.; Peña, D.; Guitián, E. *Angew. Chem., Int. Ed.* **2012**, *51*, 173. (c) Okamoto, T.; Mitsui, C.; Yamagishi, M.; Nakahara, K.; Soeda, J.; Hirose, Y.; Miwa, K.; Sato, H.; Yamano, A.; Matsushita, T.; Uemura, T.; Takeya, J. *Adv. Mater.* **2013**, *25*, 6392.
- (9) (a) Zhang, L.; Fonari, A.; Zhang, Y.; Zhao, G.; Coropceanu, V.; Hu, W.; Parkin, S.; Brédas, J.-L.; Briseno, A. L. *Chem.—Eur. J.* **2013**, *19*, 17907. (b) Zhang, L.; Walker, B.; Liu, F.; Colella, N. S.; Mannsfeld, S. C. B.; Watkins, J. J.; Nguyen, T.-Q.; Briseno, A. L. *J. Mater. Chem.* **2012**, *22*, 4266.
- (10) Clar, E. *J. Chem. Soc.* **1949**, 2013.
- (11) Malkin, J. *Photophysical and Photochemical Properties of Aromatic Compounds*; CRC Press: Boca Raton, FL, 1992.
- (12) Stein, T.; Eisenberg, H.; Kronik, L.; Baer, R. *Phys. Rev. Lett.* **2010**, *105*, 266802.
- (13) Kaur, I.; Jia, W.; Kopreski, R. P.; Selvarasah, S.; Dokmeci, M. R.; Pramanik, C.; McGruer, N. E.; Miller, G. P. *J. Am. Chem. Soc.* **2008**, *130*, 16274.
- (14) Maliakal, A.; Raghavachari, K.; Katz, H.; Chandross, E.; Siegrist, T. *Chem. Mater.* **2004**, *16*, 4980.
- (15) (a) Anthony, J. E.; Eaton, D. L.; Parkin, S. R. *Org. Lett.* **2001**, *4*, 15. (b) Anthony, J. E.; Subramanian, S.; Parkin, S. R.; Park, S. K.; Jackson, T. N. *J. Mater. Chem.* **2009**, *19*, 7984.
- (16) Inokuchi, H.; Saito, G.; Wu, P.; Seki, K.; Tang, T. B.; Mori, T.; Imaeda, K.; Enoki, T.; Higuchi, Y.; Inaka, K.; Yasuoka, N. *Chem. Lett.* **1986**, *15*, 1263.
- (17) Coropceanu, V.; Li, H.; Winget, P.; Zhu, L.; Brédas, J.-L. *Annu. Rev. Mater. Res.* **2013**, *43*, 63.
- (18) (a) Salman, S.; Ruiz Delgado, M.; Coropceanu, V.; Brédas, J.-L. *Chem. Mater.* **2009**, *21*, 3593. (b) Liuolia, V.; Valkunas, L.; Grondelle, R. *J. Phys. Chem. B* **1997**, *101*, 7343.